Anamorphic concentration of solar radiation beyond the one-dimensional thermodynamic limit

Nir Davidson, Lev Khaykovich, and Erez Hasman

We propose and demonstrate a new scheme for anamorphic concentration of a big (40 cm × 40 cm) diffuse light source to achieve an extremely high concentration in one lateral direction at the expense of that in the other direction, to preserve the total (two-dimensional) optical brightness. Such anamorphic concentration is achieved by a combination of two conventional two-dimensional concentrators and a properly designed retroreflector array. Our experiments in search of a diffuse white-light source with properties comparable with those of solar radiation have yielded 28-fold improvement of the one-dimensional concentration ratio compared with those of conventional concentrators and 14-fold improvement compared with the one-dimensional thermodynamic limit. © 2000 Optical Society of America

OCIS codes: 080.2740, 220.1770, 230.6080, 350.6050.

1. Introduction

The concentration of solar radiation or other diffuse-light sources in a single lateral direction is required for many applications. Such applications include the concentration of solar radiation into narrow water pipes for water-heating systems and the excitation of photochemical reactions[1,2] and side pumping of solar-pumped lasers.[3] Applications for other diffuse sources include efficient formation of narrow light lines in optical scanners, faxes, and copy machines, for optical metrology,[4] and for high-resolution grating-based spectrometers.[5]

For such applications a one-dimensional concentration in so-called two-dimensional concentrators,[2] which range from simple imaging concentrators such as cylindrical lenses and cylindrical parabolic mirrors to more-efficient nonimaging concentrators,[2] has been proposed. In these two-dimensional concentrators light is manipulated in one transverse direction only; hence these concentrators are subjected to the one-dimensional version of etendue (or optical brightness) invariance and only concentrate light by a factor of $\sim 1/\sin\alpha_x$, where α_x is the incoming divergence angle in the concentration direction.[1] This limit is much smaller than the thermodynamic limit on the concentration ratio, $\sim 1/(\sin\alpha_x)^2$, that is achieved with three-dimensional concentrators.[1]

In this paper we present an approach to using the anamorphic concentration of solar energy in particular and of diffuse light in general to achieve an extremely high concentration of energy in one lateral direction at the expense of that in the other direction. It is based on the use of two conventional two-dimensional concentrators and a tilted retroreflector array that performs the necessary coupling between the two transverse directions. We show theoretically and experimentally how this approach can achieve concentrations close to the thermodynamic limit. Furthermore, its simplicity and robustness to most aberrations enables us to build and test a relatively large (40 cm × 40 cm) anamorphic concentrator by using a diffuse polychromatic (white) source with characteristics similar to those of solar radiation, which still perform close to the theoretical limit.

Several techniques for anamorphic transformation that use optical fibers,[6] diffractive optical elements,[7,8] and arrays of micro-optical components[9–11] have been proposed. However, these elements are typically limited to small-optics applications, and it may be difficult to extend them to sizes of many centimeters or to operate with a wide-spectrum source. Indeed, all these transformations[6–11] were used to concentrate linear diode laser bars into symmetrical spots, whereas our anamorphic transformation uses a large

N. Davidson (fedavid@wis.weizmann.ac.il) and L. Khaykovich are with the Department of Physics of Complex Systems, Weizmann Institute of Science, Rehovot 76100, Israel. E. Hasman is with the Optical Engineering Group, Faculty of Mechanical Engineering, Technion—Israel Institute of Technology, Haifa 32000, Israel.

Received 3 January 2000; revised manuscript received 20 March 2000.

0003-6935/00/220001-05$15.00/0

© 2000 Optical Society of America

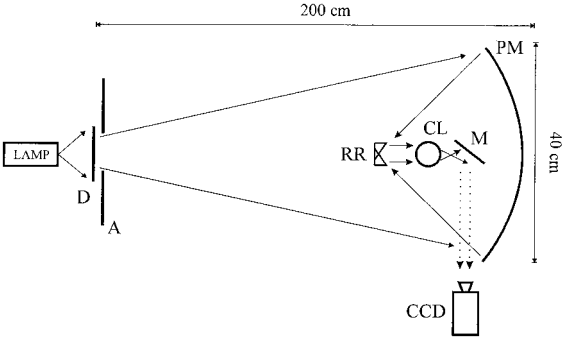

Fig. 1. Experimental optical arrangement for one-dimensional concentration of a large (40-cm) diffuse source: D, diffuser; A, aperture, M, mirror; other abbreviations defined in text.

and polychromatic diffuse source to perform the inverse (or time-reversal) operation.

2. Design Procedure

Our optical arrangement for the one-dimensional concentration of a large diffuse light source is illustrated in Fig. 1. It consists of three simple steps: (i) Focus in the X direction with a cylindrical parabolic mirror (PM), (ii) interchange the divergence angles in the X and Y directions (without changing their sizes) with a linear array of square one-dimensional retroreflectors oriented at 45° to the X and Y axes, and (iii) focus again in the X direction with a cylindrical lens (CL).

The principle of our anamorphic transformation is illustrated in Fig. 2. Figure 2(a) shows the diffuse-light source. The dimensions $D_{X1} = D_{Y1}$ are determined by the size of the source, and the lengths of the double arrows represent divergence angles $\alpha_{X1} = \alpha_{Y1}$.[12] We continue to use this graphic notation to represent the (four-dimensional) spatial and angular light distribution at subsequent cross sections [Figs. 2(b)–2(d)]. The light distribution at the focal plane of the PM is shown in Fig. 2(b). Now the size of X is much smaller then the size of Y but has a larger divergence angle. The light distribution immediately after retroreflection is shown in Fig. 2(c). As can be seen, for each small local retroreflector (RR) both size and divergence are transposed in the X and Y directions. The size of the local square RR is chosen to match the X size of the focused beam exactly, so the local sizes are actually unchanged on retroreflection. Hence, for the entire input, the X and Y divergences are transposed, whereas the total X and Y sizes are unchanged. Therefore, after reflection from the RR array, the total X size is much smaller then the total Y size and also has much smaller divergence angles. Therefore the beam can be concentrated again in the X direction with a cylindrical lens [Fig. 2(d)].

3. Experimental Procedure and Results

Here we describe in more detail the three parts of the optical arrangement of Fig. 1: the diffuse-source preparation, the concentrator, and the detection. To

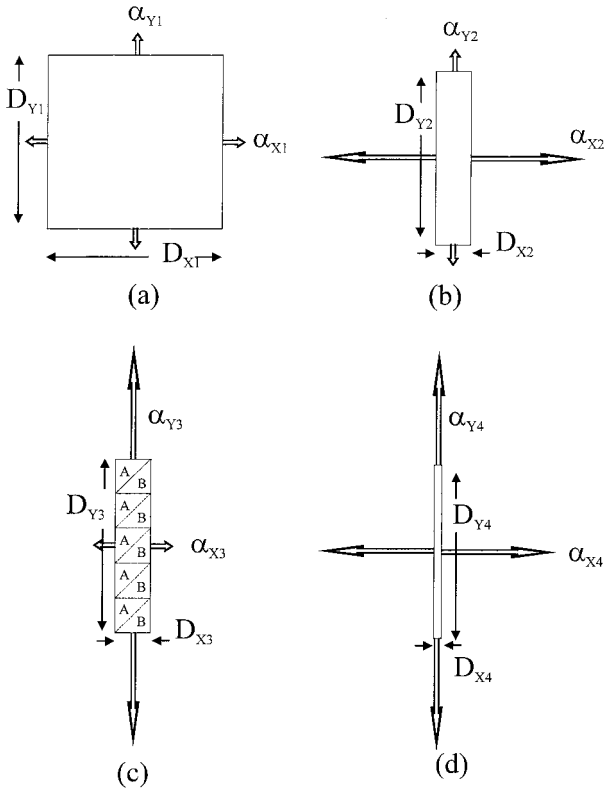

Fig. 2. Illustrations of spatial and angular light distributions at several planes along the optical axis of the anamorphic concentrator (Fig. 1). The width and the height of the rectangle represent the dimensions of the beam in the X and the Y directions, respectively, and the lengths of the double arrows represent the divergence angles in the respective directions (a) at the input, (b) at the back focal plane of the parabolic reflector, before retroreflection, (c) after retroreflection (a projection of the one-dimensional retroreflector array is also shown for orientation), and (d) at the back focal plane of the cylindrical lens.

simplify the notation we use the paraxial approximation $\alpha \cong \sin\alpha \cong \tan\alpha$ for the small incoming divergence angles (but not for the large angles after concentration). We also employ only geometrical optics, because for our experiments the diffraction-limited angles and spot sizes are much smaller than the diffusive ones.

A. Preparation of a Diffuse White Source

An effective diffuse source with characteristics similar to those of solar radiation is prepared with a white-light xenon arc-lamp that has a continuous spectrum covering the entire visible range. The lamp illuminates a diffuser adjacent to a square aperture with diameter $D_0 = 4$ cm that is located $L = 200$ cm away from the PM. We define the effective source as the light distribution at the plane of the PM (of course most of the light from the lamp is either blocked by the square aperture or scattered by the diffuser outside the PM aperture). The size of our effective source is therefore the size of the PM, $D_{X1} = D_{Y1} = 40$ cm, and its (half) local divergence angles are $\sin\alpha_{X1} = \sin\alpha_{Y1} \cong D_0/2L = 0.01$. Note that

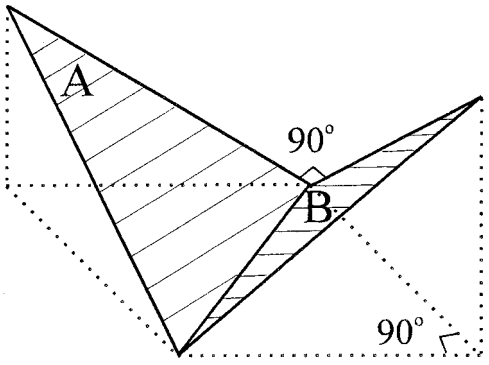

Fig. 3. Perspective drawing of a single square RR from the array shown in Fig. 2(c) composed of two orthogonal reflecting triangles (A and B) tilted at 45° to the X and Y axes, respectively.

these divergence angles are ~2 times larger than for solar radiation on Earth.

B. Concentration

We constructed a homemade 40 cm by 40 cm PM by gluing a thin aluminum reflector (measured reflectance, 87%) to a one-dimensional parabolic support structure formed by a computer-controlled lathe with the shape $Z(X, Y) = X^2/4F$, where $F = 24$ cm is the focal distance of the PM. The numerical aperture of the PM was hence 0.7, which is the optimal value for diffuse-light concentration,[1] given the requirement for 100% collection efficiency.[13] It yields a one-dimensional X concentration of $1/(2 \sin\alpha_{X1})$, which is best for any imaging concentration and is only a factor of 2 from the one-dimensional thermodynamic limit $1/\sin\alpha_{X1}$.[1] We checked the performance of the PM with a nearly collimated source (which we obtained by setting the diameter of the source aperture to $D_0 = 1$ mm). The measured X size of ~1 mm was a result of imperfections in the parabolic shape and of a small spherical aberration that resulted from the finite distance of the source. Note that chromatic aberrations, which are a major problem with refractive elements, are completely suppressed here. For our diffuse source, the beam's X size at the focus of the PM was then $D_{X2} = 2D_{X1}\sin\alpha_{X1} = 8$ mm, and its X divergence angle was $\sin\alpha_{X2} = 0.7$. In the Y direction nothing has changed; hence $D_{Y2} = D_{Y1} = 40$ cm and $\sin\alpha_{Y2} = \sin\alpha_{Y1} = 0.01$ (we neglect a slight increase $F\sin\alpha_{Y1} = 0.4$ cm that is due to free-space propagation for a distance F). Note that the optical brightness in each direction is conserved.

The RR array, located at the focal distance of the PM, is composed of 40 square 1 cm by 1 cm one-dimensional RR's rotated at 45° to the X and Y axes. Each square RR is composed of two reflecting triangular planes, as shown in Fig. 3 [their projections in the XY plane are marked as triangles A and B in Fig. 2(c)]. The 80 triangles were made from the same thin reflecting aluminum as the PM and were also glued to a support structure formed by a computer-controlled lathe. They were cut with a lathe (20 at a time) stacked between thick aluminum plates to prevent stress-induced mechanical distortion. We measured the accuracy of the 90° corner by retroreflecting a collimated laser beam and found it to be ~0.01 rad. As we explained above, each 45° RR locally transposes both beam size and divergence between the X and Y directions. However, inasmuch as the local beam size is symmetric (~1 cm by ~1 cm) and the divergence angles are not, the net function of the RR array is to maintain the global X and Y beam sizes ($D_{X3} = D_{X2} = 1$ cm and $D_{Y3} = D_{Y2} = 40$ cm) but to transpose the global divergence angles ($\sin\alpha_{X3} = \sin\alpha_{Y2} = 0.01$ and $\sin\alpha_{Y3} = \sin\alpha_{X2} = 0.7$). Unlike in our previous design for the RR array,[5] here we obtained almost no increase in beam X size by using the RR.[14]

After reflection from the RR array the beam is again focused in the X direction by a glass circular rod (cylinder) with a 12-mm diameter and a 40-cm length. The total aberrations of the glass rod when it is illuminated with a 10-mm-wide white collimated source (effective numerical aperture, ~0.8) were measured to be ~100 μm, and its transmittance was ~90% (owing to Fresnel reflections).

C. Detection

A 40 cm by 1 cm diffuser mounted upon a Z translation stage was placed at the focal plane of the glass rod (approximately 1 mm behind it). The light distribution of the diffuser was folded by a 45° narrow mirror and imaged to a calibrated CCD camera connected to a frame grabber and a computer. The resolution of the imaging system was verified to be better than 50 μm.

D. Results

Figure 4 shows sections of the light-intensity distributions imaged with the CCD camera at the output of our anamorphic concentrator and at the focus of the PM (i.e., after the first concentration stage). More quantitatively, Fig. 5 shows the measured X cross section of the light-intensity distribution at those planes. We believe that the width of 8.4 mm (FWHM) obtained at the PM focal plane represents the largest one-dimensional concentration that is possible with an imaging isotropic concentration (and is a factor of 2 less than the one-dimensional thermodynamic limit that can be obtained with nonimaging concentration). Also shown is the X cross section of the light distribution at the output plane of our anamorphic concentrator, which has a width of 0.3 mm (FWHM); this represents a 28-times-larger one-dimensional concentration than the PM (and a 14-times-larger concentration than the one-dimensional thermodynamic limit). The Y size at both planes was still 40 cm, but the Y divergence of the beam after the anamorphic concentration was much larger then after the PM, as is of course necessary to ensure conservation of the total (two-dimensional) beam brightness.

The total throughput of our setup was ~50%, which resulted from an ~5% loss owing to blocking of the incoming beam by the RR array, an ~13% loss for

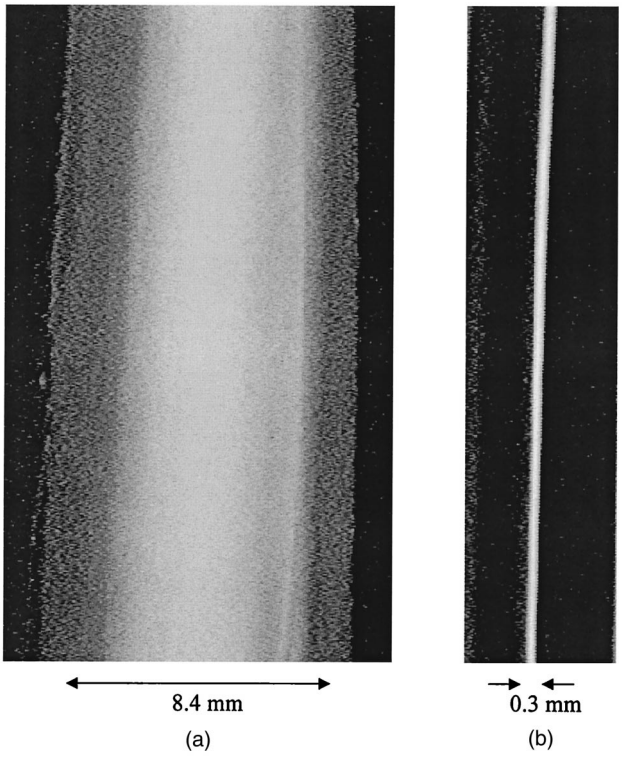

Fig. 4. Sections of the light-intensity distributions imaged with a CCD camera (a) at the focus of the parabolic mirror of Fig. 1 and (b) at the output of the anamorphic concentrator with the arrangement shown in Fig. 1.

each aluminum surface, and the ~10% Fresnel-reflection loss of the CL. Using higher reflection surfaces and applying an antireflection coating to the CL should increase the throughput to >90%.

In the absence of any aberrations and imperfections, the X size for our concentrator would be 0.15 mm, ~2 times smaller then the actual experimental result. The main contribution to the experimental increase comes from light rays that impinge upon the CL with large α_Y. The rays are then focused at a distance $f \sin\alpha_Y$, where f is the effective focal length of the CL. We calculated this inclination effect numerically for the parameters of our experiment and obtained a spot size in good agreement with the observed one. To verify this explanation further we also used the same glass rod to concentrate a beam with the same X properties but well collimated in the Y direction. The measured spot size was indeed ~2 times smaller, as expected because of the absence of the inclination effect here. This result indicates that even a perfect CL (i.e., one without any spherical or chromatic aberrations) is not an optimal X concentrator for light with large divergence angles in the Y direction. However, this reduction in concentration is rewarded with the extreme simplicity of being able to use a simple glass rod.

For still better concentration one may use a one-dimensional nonimaging concentrator instead of the glass rod and obtain concentrations that approach the thermodynamic limit.[1] Note that, in comparison with the inclination aberrations discussed above, all other aberrations in our setup, from the PM, the RR array, normal aberrations of the CL, and various alignment errors, are negligible.

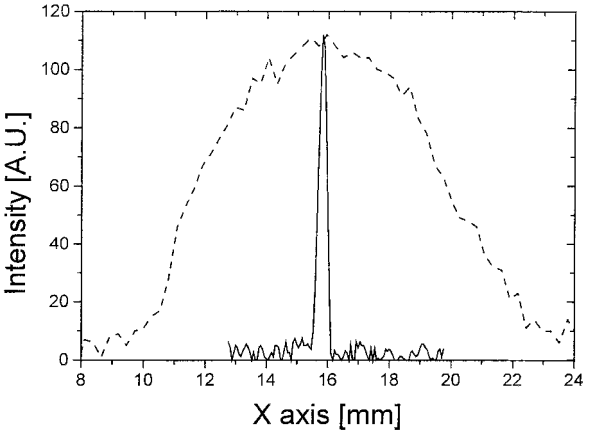

Fig. 5. Measured X cross section of the light-intensity distributions at the output of the large anamorphic concentrator with arrangement shown in Fig. 1 (solid curve) and at the back focal plain of the parabolic mirror of Fig. 1 (dashed curve).

4. Conclusions

We have demonstrated anamorphic concentration of a large (40 cm by 40 cm) diffuse source with an extremely high concentration of ~1300 in one direction (and no concentration in the other direction). The suppression of all chromatic aberrations in the first concentration stage by reflection optics makes it suitable for use with a large polychromatic source, such as solar light. The optical setup contains two standard and simple optical elements (a parabolic mirror and a glass rod) and a relatively simple array of one-dimensional retroreflectors. We believe that this simplicity can facilitate upscaling of this or similar setups to sizes of many meters that can be more useful for large solar facilities. Finally, our concept may also be applied to cases in which the diffuse source is anisotropic, as occurs, for example, for solar concentration with one-axis tracking only (where the effective source extends over 47° in the north–south direction and 0.53° in the east–west direction).[15] There it can either replace or supplement other two-stage concentration concepts[15] that aim to optimize the concentration in each direction separately and thus approach the two-dimensional thermodynamic limit. The ability of our configuration to increase the beam brightness in one direction (at the expense of brightness in the other direction) will then permit the shape of the concentrated beam to be adapted to any required application (e.g., a line, a linear array of symmetric spots as in Ref. 15, or one symmetric spot).

References and Notes

1. R. Winston and W. T. Weldford, *High Collection Nonimaging Optics* (*Academic, New York, 1989*).
2. R. Winston, I. M. Bassett, W. T. Welford, and R. Winston, "Nonimaging optics for flux concentration," in *Progress in Op-*

tics, E. Wolf, ed. (North-Holland, Amsterdam, 1989), Vol. 27, pp. 161–226.
3. I. Pe'er, N. Naftali, and A. Yogev, "High-power solar-pumped Nd:YAG laser amplifier for free-space laser communication," in *Nonimaging Optics: Maximum Efficiency Light Transfer IV*, R. Winston, ed. Proc. SPIE **3139,** 194–204 (1997).
4. E. Hasman, S. Keren, N. Davidson, and A. A. Friesem, "Three-dimensional optical metrology with color-coded extended depth of focus," Opt. Lett. **24,** 439–441 (1999).
5. N. Davidson, L. Khaykovich, and E. Hasman, "High-resolution spectrometers for diffuse light using anamorphic concentration," Opt. Lett. **24,** 1835–1837 (1999).
6. Th. Graf and J. E. Balmer, "High-power Nd:YLF laser end pumped by a diode-laser bar," Opt. Lett. **18,** 1317–1319 (1993).
7. J. R. Leger and W. C. Goltsos, "Geometric transformation of linear diode-laser arrays for longitudinal pumping of solid state lasers," IEEE J. Quantum Electron. **28,** 1088–1100 (1992).
8. N. Davidson and A. A. Friesem, "Concentration and collimation of diffuse linear light source," Appl. Phys. Lett. **62,** 334–336 (1993).
9. S. Yamaguchi, T. Kobayashi, Y. Saito, and K. Chiba, "Collimation of emissions from a high-power multistripe laser-diode bar with multiprism array coupling and focusing to a small spot," Opt. Lett. **20,** 898–900 (1995).
10. B. Ehlers, K. Du, M. Baumann, H.-G. Treusch, P. Loosen, and R. Poprawe, "Beam shaping and fiber coupling of high-power diode laser arrays," in *Lasers in Material Processing*, L. H. Beckmann, ed., Proc. SPIE **3097,** 639–644 (1997).
11. M. Baumann, B. Ehlers, M. Quade, K. Du, H.-G. Treusch, P. Loosen, and R. Poprawe, "Compact fiber-coupled high-power diode-laser unit," in *Lasers in Material Processing*, L. H. Beckmann, ed., Proc. SPIE **3097,** 712–716 (1997).
12. To simplify the notation, we discuss the special case when $D_{X1} = D_{Y1}$ and $\alpha_{X1} = \alpha_{Y1}$. The procedure is applicable also to the general case $D_{X1} \neq D_{Y1}$ or $\alpha_{X1} \neq \alpha_{Y1}$.
13. Our procedure can be readily extended for broader optimization criteria when the flux concentration can be increased in exchange for a small sacrifice in collection efficiency. This would lead to higher optimal values for the numerical aperture of the PM, depending on the exact trade-off between concentration and efficiency.
14. Because the actual X width of the beam at the RR plane was measured to be 8.4 mm (FWHM), slightly larger than the theoretical value, we used a 10-mm size for each RR to reduce clipping losses to $<2\%$. This yielded an increase in the beam X size to 10 mm on retroreflection.
15. M. Brunotte, A. Goetzberger, and U. Blieske, "Two-stage concentrator permitting concentration factors up to 300× with one-axis tracing," Solar Energy **56,** 285–300 (1996).